Contribution from E.R. No. 139 du C.N.R.S., Université L. Pasteur, 67008 Strasbourg Cédex, France

Intramolecular Rearrangements in Trifluorophosphorane. An ab Initio LCAO–MO–SCF Study

ALAIN STRICH

Received August 3, 1977

Dynamic NMR experiments have indicated that trifluorophosphorane PH_2F_3 rearranges intramolecularly through modes M_2 or M_4. Ab initio LCAO–MO–SCF calculations are here reported for eight stereoisomers of this molecule: a half-twisted trigonal bipyramid, a distorted TBP, the three possible TBP's, and the three possible tetragonal pyramids. The first two structures whose geometries were partially optimized are assumed to intervene on the pathway of the one-step rearrangement mechanisms corresponding to modes M_2 and M_4; the other six, whose geometries were optimized, intervene on the pathway of the multistep mechanisms consisting in a succession of Berry pseudorotations. The calculated geometry of the ground-state TBP is in very good agreement with experimental evidence. The relative stabilities of the stereoisomers are rationalized. The lowest energy pathway for intramolecular rearrangement is found to be the multistep mechanism corresponding to mode M_4 with a barrier of 8.6–9.6 kcal mol^{-1}. The heights of the barriers to intramolecular rearrangement of the PY_2F_3 phosphoranes (Y = F, CF_3, Cl, Br, H, Me, Ph, NMe_2) are rationalized on this basis.

Introduction

Intramolecular ligand exchange in fluorophosphoranes PY_nF_{5-n} has been extensively studied by means of dynamic NMR spectroscopy.[1] For trifluorophosphoranes PY_2F_3, the coalescence of the signals of axial and equatorial fluorine nuclei on increasing the temperature has been accounted for in terms of intramolecular rearrangement modes[8,18] (see ref 22 for a discussion and classification of rearrangement modes). For such molecules, it is impossible, on the basis of the temperature-dependent NMR spectra, to distinguish between modes M_2 (ae process) and M_4 (aae process). These two modes are represented on Figure 1 for PH_2F_3. They are the only ones keeping two fluorine atoms in axial position and making the three fluorine atoms equivalent. As is well known, the rearrangement modes are merely permutational in character and do not contain any information regarding the mechanistic pathway by which a species proceeds from the initial to the final stereoisomer.

For PH_2F_3, it has been stated that the rearrangement might proceed via either one-step or multistep processes consistent with the (M_2, M_4) modes.[9] The one-step process for mode M_2(ae) is represented in Figure 2.

The geometrical midpoint between the initial and the final trigonal bipyramids (TBP1) is a half-twisted TBP (HTTBP); F_a and F_e have been rotated by 90° about the C_2-axis bisector of $\angle F_aPF_e$ in TBP1. In this hypothesis the barrier to intramolecular rearrangement is the energy difference between the two structures HTTBP and TBP1 (if the HTTBP structure corresponds to the transition state as in **1**, otherwise this energy

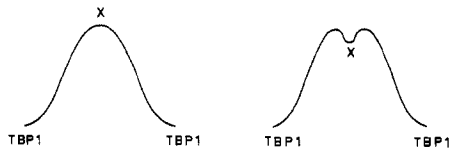

1 **2**

difference represents a lower limit to the barrier if the HTTBP structure is a reaction intermediate as in **2**, X = HTTBP). The one-step process for mode M_4 (aae) is represented in Figure 3. The geometrical midpoint between the initial and the final stereoisomers is a distorted TBP (DTBP): four atoms are coplanar (the two H, P, and F_a), F_e and F_a' are symmetric with respect to that plane. In this hypothesis the barrier to intramolecular rearrangement is the energy difference between the two structures DTBP and TBP1 (with the same remarks as above, see **1** and **2** with X = DTBP).

We have considered two multistep processes. Both consist of a succession of Berry pseudorotations[23] (BPR) which interconvert two TBP structures via a tetragonal pyramid (TP) structure.[24] Axial and equatorial ligands are exchanged pairwise, whereas one ligand, the so-called "pivot" of the BPR remains in equatorial position. The reasons for the choice of the BPR as the elementary step in a multistep process are the following: (i) for phosphoranes, the BPR mechanism has been shown to be energetically much easier than the turnstile rotation (TR) mechanism,[25] on the basis of MO calculations, at the extended Hückel,[26] CNDO,[25,27] or ab initio SCF level;[28,29] (ii) it is consistent with the NMR line-shape analysis for tetrafluorophosphoranes;[12,30] (iii) it takes a specific account of the close relationship between the TBP and TP stereochemistries; (iv) the structural distortions of cyclic phosphoranes have been shown to form a continuous series between the idealized TBP and TP structures, and these findings reinforce the operation of successive BPR's postulated to account for NMR exchange data on a wide variety of phosphoranes.[29]

Scheme I

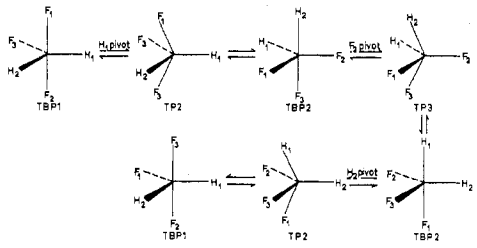

Scheme II

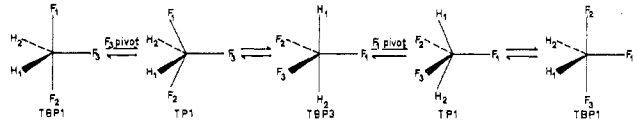

The two multistep processes are represented in Schemes I and II. The labels of the different stereoisomers are also defined in the schemes. (i) The overall process depicted in Scheme I corresponds to mode M_2 since the initial and final TBP1's differ by an ae permutation (namely F_1 and F_3). (ii) Scheme II corresponds to mode M_4 (aae permutation). (iii) For Scheme I, e.g., we have arbitrarily chosen H_1 as the pivot in the first BPR; we might have taken H_2, the final result would not have been changed. The same arguments hold for all BPR's where several alternatives are possible for the choice of the pivot. (iv) In the hypothesis of multistep processes, the barrier to intramolecular rearrangement of PH_2F_3 is calculated as the energy difference between the stereoisomer of highest

0020-1669/78/1317-0942$01.00/0

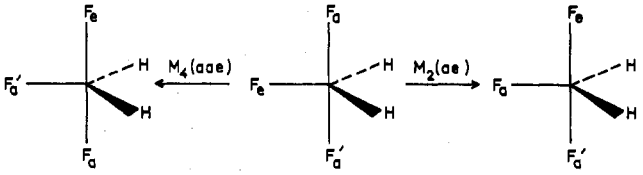

Figure 1. The two rearrangement modes, M_2 and M_4, of PH_2F_3.

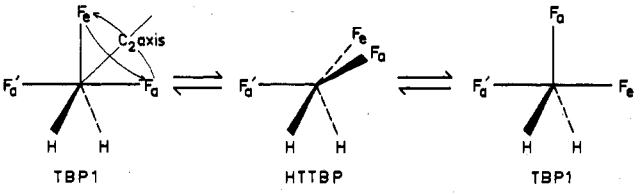

Figure 2. The one-step process for intramolecular rearrangement of PH_2F_3 according to mode M_2(ae).

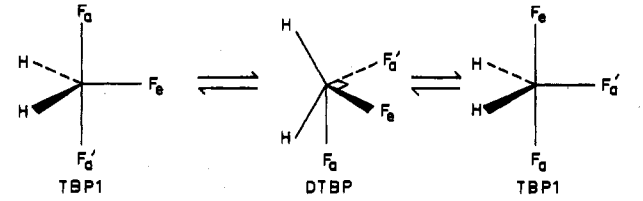

Figure 3. The one-step process for intramolecular rearrangement of PH_2F_3 according to mode M_4(aae).

energy on the pathway and TBP1.

Calculations

In order to assess which of the four above-described mechanisms might be responsible for the intramolecular rearrangement of PH_2F_3, we have undertaken a series of ab initio LCAO–MO–SCF calculations for this molecule. In a previous paper,[28] we had reported calculations for some stereoisomers of PH_2F_3, but we had not considered all of them. Furthermore no geometry optimization had been performed. Now it has been shown that for the calculation of small or relatively small barriers (as is the case here), geometry optimization was important.[32] In this work, all the geometrical parameters of most of the stereoisomers have been optimized (see below).

The calculations were carried out with the system of programs Asterix.[33] Three Gaussian basis sets (BS I, II, III) of increasing sophistication were used. They are summarized in Table I. The geometry optimizations were performed with BS II. This basis set has proved to be adequate for geometry search since it reproduced with an excellent agreement the experimental bond lengths of PF_5.[28] The inclusion of a set of d functions in the second-row atom basis set, as is the case in BS II, has been shown to be essential for the description of geometries and binding energies of hypervalent molecules,[39] such as PH_2F_3 studied in this work. BS I and BS III were used only for some optimized geometrical structures resulting from calculations with BS II. A representative timing for a calculation on TBP1 when using BS II is 4 min 19 s of CPU time for the integral computation and 30 s of CPU time for each SCF iteration (about four iterations needed) on a Univac 1110 monoprocessor. Furthermore, in a geometry search, an appreciable amount of computer time may be saved since the program does not recalculate integrals which remain invariant from a previous point on the potential energy surface.

The results of geometry optimizations together with the energies of the various stereoisomers are reported in Table II. The number of optimized geometrical parameters, N, appears in column 3. On one hand, for HTTBP, DTBP, and TP1, we have limited this number to respectively 2, 0, and 0. We shall comment on this choice in the next paragraph. On the other hand, as we expected that TBP1, TBP2, TBP3, TP2, and TP3 would lie in a rather narrow spectrum of energy, we optimized them fully, and in some cases, N reaches a rather large value.

Table I. Gaussian Basis Sets

BS I	(10, 6/8, 4/4)[a]	contracted to [6, 4/4, 2/2]
BS II	(10, 6, 1/8, 4/4)[a,b]	contracted to [6, 4, 1/4, 2/2]
BS III	(12, 9, 2/10, 6, 1/5, 1)[c,d]	contracted to [6, 4, 2/4, 2, 1/2, 1][e]

[a] References 34 and 35. [b] Exponent of the d-type function = 0.57 (optimized for PF_5).[28] [c] References 36 and 37. [d] Exponents of d-type functions: 0.8 and 0.3 on P, 1.23 on F.[38] Exponent of p-type function on H, 0.75.[38] [e] For phosphorus, contraction no. 9 of ref 36 was adopted.

Discussion

(1) The Relative Stabilities of the Stereoisomers and the Mechanisms for Intramolecular Exchange. The labels of the ligands and of the angles of the various stereoisomers referred to in this paragraph are defined on the figures of Table II.

As expected, we find (using whatever basis set) that the most stable stereoisomer is TBP1, which is the experimental ground-state geometry. No structural data are available for PH_2F_3, but its infrared spectrum,[40,41] its low-temperature NMR spectra,[9,41] and comparison with electron diffraction data for the analogous compound Me_2PF_3[42] infer an experimental ground-state geometry with the TBP1 structure, the two hydrogen atoms being in equatorial positions.

For HTTBP and DTBP, which are respectively the geometrical midpoints of the one-step ae (Figure 2) and aae (Figure 3) mechanisms, the geometrical parameters which do not vary during the course of the mechanism were fixed at their optimized value in TBP1: respectively PF′ and PH bond lengths and angle δ in HTTBP; PF′ and PH bond lengths and angles α and β in DTBP. The other parameters were taken halfway of their optimized values in the two interconverted TBP1's: PF bond length and angle γ in HTTBP and DTBP.

For HTTBP, the angles α and β were optimized. It seems reasonable to assume that they are the most important geometrical parameters (with respect to energy). Their optimization leads to a structure which somewhat resembles the transition-state structure of a TR mechanism, with $\alpha = 84.7°$ to be compared with $\theta_2 = 85°$ and $\beta = 92.4°$, $\delta = 90°$ to be compared with $\theta_3 = 95°$ (θ_2 and θ_3 being defined on page 5578 of ref 28, with their optimized values for PF_5[28]). The relative energy of 46.8 kcal mol^{-1} of HTTBP with respect to TBP1 is high and will not be significantly lowered by further optimization, so as to become competitive with the relative energies of the TBP and TP stereoisomers of Table II. This high value rules out the one-step ae mechanism of Figure 2 as a possibility for the intramolecular ligand exchange in PH_2F_3.

For DTBP, none of the geometrical parameters was optimized. This stereoisomer was calculated only for the sake of completeness. Its very high energy of 225 kcal mol^{-1} relative to TBP1 is due to the assumption of a chemically unfeasible structure with an F′PH angle of 30°. A full geometry optimization of DTBP will probably lead to a structure very close to the C_s structure of Table VI of ref 28, with a local C_2 axis exchanging the two hydrogen atoms superposed to a local C_3 axis exchanging the three fluorine atoms; still this structure with local symmetries remains higher in energy (29.1 kcal mol^{-1} relative to TBP1) than any of the TBP or TP structures reported in Table II. So the one-step aae mechanism of Figure 3 should also be ruled out as a possibility for the intramolecular ligand exchange in PH_2F_3.

Before turning to a quantitative discussion of the multistep mechanisms of Schemes I and II, a few comments on the

Table II. Optimized Geometries and Energies of the Stereoisomers of PH_2F_3

Stereoisomer[a]	Symmetry constraint	N^b	Geometry[c]		BS	$-E_{total}$[e]	Relative energy[f]
HTTBP 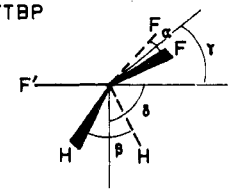	C_s	2	PF = 1.586[d] PH = 1.368[d] β = 92.4 δ = 90.0[d]	PF′ = 1.610[d] α = 84.7 γ = 45.0[d]	I II III	640.0070	46.8
DTBP 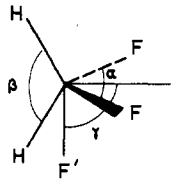	C_s	0	PF = 1.586[d] PH = 1.368[d] β = 120.0[d]	PF′ = 1.610[d] α = 90.0[d] γ = 90.0[d]	I II III	639.7233	225
TBP1 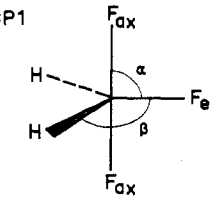	C_{2v}	5	PF_{ax} = 1.610 PH = 1.368 β = 117.5	PF_e = 1.562 α = 90.6	I II III	639.9320 640.0816 640.2921	0.00 0.00 0.00
TBP2 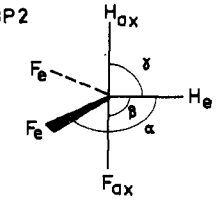	C_s	5	PF_{ax} = 1.595 PH_{ax} = 1.394 α = 120.3 γ = 90.0[d]	PF_e = 1.567 PH_e = 1.384 β = 90.0[d]	I II III	639.9035 640.0625 640.2774	17.9 12.0 9.17
TBP3 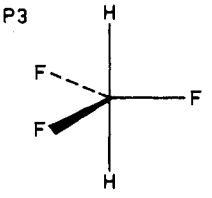	D_{3h}	2	PF = 1.586	PH = 1.378	I II III	639.9119 640.0667 640.2784	12.6 9.31 8.57
TP1 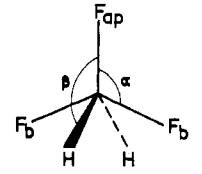	C_{2v}	0	PF_{ap} = 1.579[d] PH = 1.375[d] β = 98.3[d]	PF_b = 1.594[d] α = 111.2[d]	I II III	640.0654 640.2767	10.2 9.63
TP2 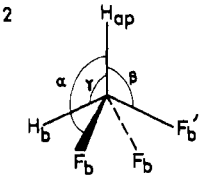	C_s	7	PF_b = 1.604 PH_{ap} = 1.366 α = 96.1 γ = 112.4	PF'_b = 1.572 PH_b = 1.375 β = 105.5	I II III	640.0726	5.63
TP3 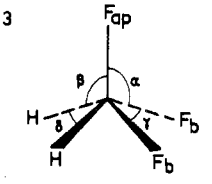	C_s	7	PF_{ap} = 1.548 PH = 1.392 β = 105.1 δ = 92.7	PF_b = 1.594 α = 100.0 γ = 86.2	I II III	640.0546 640.2699	16.9 13.9

[a] In a TBP ax = axial, e = equatorial; in a TP ap = apical, b = basal. [b] Number of optimized geometrical parameters. [c] Bond lengths in Å, angles in degrees. [d] Fixed (see text). [e] Total energy in atomic units. [f] With respect to TBP1 (in kcal mol^{-1}).

Table III. Atomic Charges of the TBP Stereoisomers of PH_2F_3 Resulting from a Mulliken Population Analysis[a]

Atom	BS	TBP1	TBP2	TBP3
P	I	+1.772	+1.809	+1.771
	II	+1.455	+1.463	+1.447
	III	+1.818	+1.830	+1.851
F_{ax}	I	−0.635	−0.609	
	II	−0.531	−0.503	
	III	−0.565	−0.560	
F_{eq}	I	−0.550	−0.555	−0.576
	II	−0.441	−0.447	−0.476
	III	−0.536	−0.541	−0.549
H_{ax}	I		−0.068	−0.021
	II		−0.065	−0.009
	III		−0.098	−0.102
H_{eq}	I	+0.024	−0.021	
	II	+0.024	0.000	
	III	−0.076	−0.090	

[a] Electrons: + for positive charge, − for negative charge.

relative stabilities of TBP and TP stereoisomers are necessary.

(i) With whatever basis set, TBP3 is found more stable than TBP2 (by respectively 5.3, 2.7, and 0.6 kcal mol^{-1} with BS I, II, and III). This result is unexpected since, on the basis of the so-called polarity rule,[43,44] in a PX_nY_{5-n} phosphorane (with X more electronegative than Y, n = 2, 3) a TBP with only one axial Y ligand is expected to be more stable than one with two axial Y ligands. This rule seems supported by Hückel-type calculations on PF_3Cl_2 and PF_2Cl_3,[45] PF_3H_2 and PF_2H_3,[26] CNDO calculations on PF_2Cl_3,[46] as well as ab initio LCAO–MO–SCF calculations on $PH_3{*}H_2$ and $PH_2{*}H_3$[47] (with H* simulating an electronegative ligand) and PF_2H_3.[48] We have also found the same trend by carrying out extended Hückel calculations on our optimized TBP2 and TBP3, whereas CNDO calculations reproduced the same order as the ab initio calculations. The only exception to the polarity rule which we could find in the literature is a CNDO calculation on PF_3H_2 where the TBP3-like structure is found more stable than the TBP2 by 0.5 kcal/mol.[25] So, of all the explicit calculations on PF_3H_2, only the ones in the extended Hückel formalism yield a sequence of stabilities which differs from ours, and the reason for this discrepancy may be found in Hoffmann's statement "the extended Hückel method is known to poorly represent highly ionic bonding".[26] This shortcoming is not present in SCF–MO methods such as CNDO or ab initio. Furthermore, it should be noticed that in TBP2, we have arbitrarily fixed β and γ at 90° (see Table II) in order to have an idealized TBP. If these angles are relaxed, one obtains the TP2 structure which is now more stable than TBP3, but whose geometry (bond lengths as well as angles) is much closer to TBP1 than to TBP2, as is apparent from Table II.

One possible reason for this nonobservance of the polarity rule is a preferential stabilization of TBP3 by formation of some kind of intramolecular

hydrogen bond. In TBP3 we have six short nonbonded $H_{ax}F_{eq}$ distances of 2.10 Å (to be compared with the H···F hydrogen bond length of 1.93 Å in $(HF)_2$[49]). The atomic charges resulting from a Mulliken population analysis are reported in Table III. With BS I and BS II, the negative charge on F_{eq} increases when going from TBP1 to TBP3, with a large gap when going from TBP2 to TBP3. Correspondingly the negative charge on H_{ax} decreases strongly from TBP2 to TBP3. This trend appears also in the conclusions of Kollman and Allen regarding charge redistribution in hydrogen bonded systems:[50] the hydrogen in the H bond loses electrons upon hydrogen bonding; the electronegative atoms gain electrons.

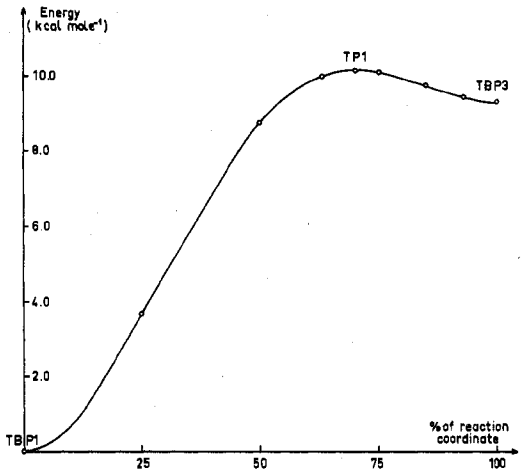

Figure 4. Reaction path from TBP1 to TBP3. O = calculated points.

This kind of intramolecular hydrogen bond would explain why, in BS I and II, TBP3 is more stable than TBP2. The above trend is not observed when using BS III; there is no appreciable change in the atomic charges of F_{eq} and H_{ax} in going from TBP2 to TBP3. This is why TBP2 lies very close in energy to TBP3 in BS III. Furthermore it is known that small basis sets generally enhance hydrogen bond energies.[51]

(ii) According to extended Hückel calculations on PH_2F_3[26] or ab initio calculations on $PH_2H_3{*}$,[47] the order of increasing energies (or decreasing stabilities) is TP2 < TP1 ~ TP3. Our order using BS II is TP2 < TP1 < TP3. The agreement is slightly better than for the trigonal bipyramids, but TP1 is found definitely more stable than TP3. The reason for the discrepancy is the same as the one noted above, the geometry of TP1 being close to the one of TBP3 which is poorly described by extended Hückel calculations. TP2 is found to lie only 5.63 kcal mol^{-1} above TBP1. Examination of the geometries of these two stereoisomers shows that the bond lengths are almost exactly identical if one compares the apical bond (whose ligand is the pivot of the BPR) of TP2 to the equatorial one of TBP1 and the two sets of opposite basal bonds of TP2 to the two sets of axial and equatorial bonds in TBP1. Actually the largest bond length difference between TP2 and TBP1 is 0.010 Å (PF'_b vs. PF_e). So TP2 differs from TBP1 only by axial and equatorial bending and appears as a vibrationally excited state of TBP1 through modes ν_6 and ν_7 which are of low energy for phosphoranes.[52]

We now turn to the discussion of the multistep rearrangement mechanisms. Using BS II, the stereoisomer of highest energy along the pathway represented by Scheme I turns out to be TP3 (16.9 kcal mol^{-1} relative to TBP1). For the pathway represented by Scheme II, the situation is the following. Starting from TBP1, the BPR leads to TBP3 via TP1. TBP1 and TBP3 belong to different point groups (respectively C_{2v} and D_{3h}) and consequently have a different number of degrees of freedom (respectively 5 and 2); so it is possible to fully optimize their geometries, which has been done. But TP1 belongs to the same point group as TBP1 and any trial to optimize it would fall on TBP1. Ideally one should search for the minimum energy pathway from TBP1 to TBP3 on a five-dimensional potential surface with a constraint of C_{2v} symmetry. But it seems reasonable to assume that a two-dimensional slice would be a good approximation, the two degrees of freedom being the α and β angles of TBP1 and TP1 (see Table II). This is actually what Hoffmann and co-workers have done for PH_5.[26] However, this procedure would still be too expensive at the level of ab initio SCF calculations. So we adopted for the reaction coordinate, a linear variation of the five degrees of freedom from TBP1 to TBP3. The resulting one-dimensional curve drawn from nine calculated points, using

Table IV. Selected Experimental and Calculated Geometrical Parameters of Some Trigonal-Bipyramidal Fluorophosphoranes[a,b]

Molecule	PF_{ax}	PF_{eq}	PH	$\angle F_{ax}PR^m$	$\angle F_{eq}PR^m$	$\angle F_{eq}PF_{ax}$
PF_5[c,d]	1.577 (5)	1.534 (4)				
PF_5[e,f]	1.571	1.542				
PF_4H[g,h]	1.594 (5)	1.55 (3)	1.36 (5)	90 (4)	124 (2)	
$PF_4(CH_3)$[c,i]	1.612 (4)	1.543 (4)		91.8 (4)	122.2 (9)	
PF_3H_2[e,j]	1.610	1.562	1.368	89.7	117.5	90.6
$PF_3(CH_3)_2$[c,i]	1.643 (3)	1.553 (6)			118.0 (8)	89.9 (3)
PF_2H_3[e,k]	1.680		1.36	90.0		
$PF_2(CH_3)_3$[c,l]	1.685 (1)					

[a] Bond lengths in Å, angles in deg. [b] In parentheses is the absolute error on the last figure in the experimental determination. [c] Experimental (electron diffraction). [d] Reference 62. [e] Calculated (ab initio LCAO-MO-SCF). [f] Reference 28. [g] Experimental (microwave). [h] Reference 63. [i] Reference 42. [j] This work (TBP1). [k] Reference 48. [l] Reference 61. [m] R = ligand other than fluorine in equatorial position.

BS II, is represented on Figure 4. For the overall mechanism of Scheme II it is of course symmetric with respect to a vertical axis passing through TBP3, thus producing a curve of type **2**. The highest TP1 is at 70% of the reaction coordinate, 10.2 kcal mol^{-1} above TBP1; this is the point which is reported in Table II and which determines the barrier of the mechanism of Scheme II. With the assumption of a linear variation of the five degrees of freedom, one is not sure that the curve of Figure 4 coincides with the minimum energy pathway which might be a curve of type **1**. But at least one gets an upper bound to the barrier height of the mechanism of Scheme II which is calculated to be comprised between 9.3 (height of TBP3) and 10.2 kcal mol^{-1}. Using BS III, the barriers of the mechanisms of Scheme I and Scheme II are lowered to respectively 13.9 and 8.6–9.6 kcal mol^{-1}. BS II seems to overestimate the energy differences between TP's and TBP's (the barrier to BPR for PF_5 has been computed to be 4.8 kcal mol^{-1} using BS II,[28] whereas the most recent "experimental estimate" of this barrier is found to lie between 3.26 and 2.84 kcal/mol[53]). So the values obtained with the largest basis set, BS III, might be more reliable. The difference between the two barriers seems sufficiently appreciable to conclude that the energetically most favorable multistep mechanism for intramolecular exchange of axial and equatorial fluorine ligands is the one represented by Scheme II. A fortiori, it is much more favorable than the one-step mechanisms of Figures 2 and 3 whose calculated barriers are very much higher. This value of 8.6–9.6 kcal mol^{-1} is in poor agreement with the experimental $\Delta H^{\ddagger}$ of 14.2 kcal/mol.[9] However one should be careful when comparing calculated barrier heights and Arrhenius activation enthalpies.[54] The finding that the process represented by Scheme II is easier than the one represented by Scheme I is not so surprising. In Scheme II, a C_{2v} symmetry constraint is maintained all along the pathway, just like in the BPR of a PX_5 or PX_4Y-type phosphorane which is known to be an energetically facile process,[1b] due to the small disturbance of the MO's on carrying out the isomerization.[55]

The mechanism proposed by Holmes to account for intramolecular exchange in the PY_2F_3 species,[1b] corresponding to an ae exchange (mode M_2), has not been considered in this study. The "transition state" which is assumed closely resembles our TP2 (though the angles he proposes differ appreciably from our optimized ones), but it seems difficult to reach it directly from TBP1 without traversing a high-energy stereoisomer, since, in the TP, the two fluorine ligands which were axial in TBP1 are now in basal cis positions, so that the ∠FPF angle has varied from 179 to 88° (considering our optimized angles).

Moreland and co-workers have compiled a series of rearrangement barriers for PF_3Y_2 phosphoranes.[18] From the $\Delta G^{\ddagger}$ values, it comes out that the barriers increase with Y in the following order: F < CF_3 < Cl ~ Br < H < Me ~ Ph ~ NMe_2. This order is in rough agreement with the order of decreasing apicophilicities given by Cavell and co-workers.[10,56] From this observation, one may conclude that for the PF_3Y_2 phosphoranes, the mechanism of Scheme II is likely to be the energetically most favorable, since a lower bound to its barrier is determined by the height of the TBP with two Y ligands in axial position.

(2) The Geometries. As mentioned earlier, no structural data are available for PH_2F_3. However, we may compare our optimized geometrical parameters with the available experimental data for related compounds. Selected calculated and experimental geometrical parameters are reported in Table IV. As shown by Yow and Bartell,[61] the variation of the PF_{ax} bond length as a function of the number of methyl substituents on a PF_5 skeleton is roughly linear. If we extrapolate linearly the PF_{ax} bond length from the experimental values in PF_5[62] and PF_4H,[63] we get 1.611 Å for PF_3H_2 which is almost exactly our optimized value in TBP1 (1.610 Å) and 1.628 Å in PF_2H_3, which is rather far from the value of 1.680 Å calculated by Keil and Kutzelnigg.[48] The same extrapolation for PF_{eq} would be more risky since the reported distance in PF_4H is within an error of 0.030 Å. However, we may see that the calculated increase (0.020 Å) in the PF_{eq} distance when going from PF_5 to PF_3H_2 is smaller than the one for the PF_{ax} distance (0.039 Å), which is in agreement with the observed trend. This trend has been explained in terms of electron pair repulsions[44] and the PF overlap populations have been recently discussed within the extended Hückel formalism.[64] Our optimized PH bond length in TBP1 is in good agreement with other available PH distances in phosphoranes (see Table IV). The $F_{eq}PH$ angle of 117.5° compares well with the $F_{eq}PC$ angle of 118.0° in $PF_3(CH_3)_2$. This has been explained in terms of larger repulsions between the PH bonding pairs.[44] The calculated $F_{eq}PF_{ax}$ angle of 90.6° is very close to its corresponding angle (89.9°) in $PF_3(CH_3)_2$.

In TBP2, TBP3, TP1, TP2, and TP3 the general structural trend of phosphoranes, according to which an axial bond is longer than an equatorial one in a TBP, and an apical bond is shorter than a basal one in a TP, is always verified. The geometries of these stereoisomers deserve no further comment. Those of HTTBP and DTBP have been discussed earlier.

Conclusion

We have reported ab initio LCAO–MO–SCF calculations on eight stereoisomers of trifluorophosphorane PH_2F_3. The geometries of two of these, namely, the halfway structures of the one-step mechanisms for intramolecular rearrangement of Figures 2 and 3, have been partially optimized (HTTBP) or assumed (DTBP). The geometries of five stereoisomers (TBP1, TBP2, TBP3, TP2, and TP3) have been fully optimized. All these geometries are consistent with the general structural trend observed in phosphoranes, namely, the axial bonds are longer than the equatorial ones in a TBP, and the apical bonds are shorter than the basal ones in a TP. We have accounted for the relative orders of stabilities obtained for TBP's and TP's. On the basis of these energies, the following

conclusions concerning the mechanism for intramolecular exchange of fluorine ligands may be drawn. The one-step mechanisms of Figures 2 and 3 may be easily ruled out because of a very high barrier. On the basis of qualitative topological arguments, Britton and Dunitz drew the conclusion that any single-step mechanism other than the one associated with the aeae rearrangement mode (i.e., the BPR) is highly improbable for a pentacoordinated molecule.[65] Among the two multistep mechanisms (consisting of a succession of BPR's) Schemes I and II, Scheme II appears as the energetically most favorable, with a barrier of 8.6–9.6 kcal mol^{-1}. This result is of importance since, on the basis of NMR line-shape analysis, no conclusion could be drawn about the mechanism but only about the modes (M_2 or M_4). Thus according to our calculations, the intramolecular rearrangement in PH_2F_3 takes place via an M_4 (aae) mode achieved through a multistep mechanism such as represented on Scheme II. On this basis, we could rationalize the fact that the order of increasing barriers to intramolecular rearrangement in PF_3Y_2 phosphoranes (Y = F < CF_3 < Cl ~ Br < H < Me ~ Ph ~ NMe_2) is parallel to the order of decreasing apicophilicities of the Y substituents.

Acknowledgment. The helpful comments of a referee are gratefully acknowledged.

Registry No. PF_5, 7647-19-0; PF_3H_2, 38474-13-4; PF_2H_3, 65451-11-8.

References and Notes

(1) (a) An extensive review covering the literature up to 1972 is R. Luckenbach, "Dynamic Stereochemistry of Pentacoordinated Phosphorus and Related Elements", G. Thieme Publishers, Stuttgart, 1973. (b) See also R. R. Holmes, *Acc. Chem. Res.*, **5**, 296 (1972). For later work, see ref 2–21.
(2) C. G. Moreland, G. O. Doak, and L. B. Littlefield, *J. Am. Chem. Soc.*, **95**, 255 (1973): Ph_2PF_3.
(3) A. H. Cowley and R. W. Braun, *Inorg. Chem.*, **12**, 491 (1973): HPF_4.
(4) E. L. Lines and L. F. Centofanti, *Inorg. Chem.*, **12**, 598 (1973): $F_4P(C{\equiv}CCH_3)$.
(5) J. W. Gilje, R. W. Braun, and A. H. Cowley, *J. Chem. Soc., Chem. Commun.*, 813 (1973): $(CF_3)PF_3H$.
(6) A. H. Cowley and J. R. Schweiger, *J. Am. Chem. Soc.*, **95**, 4179 (1973): PF_4NH_2.
(7) D. U. Robert, D. J. Costa, and J. G. Riess, *J. Chem. Soc., Chem. Commun.*, 745 (1973); J. G. Riess and D. U. Robert, *Bull. Soc. Chim. Fr.*, 425 (1975); D. U. Robert, D. J. Costa, and J. G. Riess, *Org. Magn. Reson.*, **7**, 291 (1975): $R^1PF_3(OR^2)$.
(8) R. Schmutzler, *J. Chem. Soc., Dalton Trans.*, 2687 (1973): $(R_2N)_nPF_{5-n}$, $R_nPF_{4-n}(NR'_2)$ (n = 1, 2), and fluoro-1,3,2,4-diazaphosphetidines.
(9) J. W. Gilje, R. W. Braun, and A. H. Cowley, *J. Chem. Soc., Chem. Commun.*, 15 (1974): PF_3H_2 and $(CF_3)HPF_3$.
(10) R. G. Cavell, D. D. Poulin, K. I. The, and A. J. Tomlinson, *J. Chem. Soc., Chem. Commun.*, 19 (1974): trifluoromethylfluorophosphoranes.
(11) D. D. Poulin and R. G. Cavell, *Inorg. Chem.*, **13**, 3012 (1974): $(CF_3)_{3-n}PF_n(NMe_2)_2$ (n = 1, 2).
(12) M. Eisenhut, H. L. Mitchell, D. D. Traficante, R. J. Kaufman, J. M. Deutch, and G. M. Whitesides, *J. Am. Chem. Soc.*, **96**, 5385 (1974): XPF_4 (X = Me_2N, Cl, Me).
(13) A. H. Cowley, R. W. Braun, and J. W. Gilje, *J. Am. Chem. Soc.*, **97**, 434 (1975): i-Pr_2NPF_4.
(14) J. A. Gibson, G. V. Röschenthaler, and R. Schmutzler, *J. Chem. Soc., Dalton Trans.*, 918 (1975): $RPF_2(pfp)$ (R = F, Me, Me_3C, Ph, Et_2N, $(Me_3Si)_2N$; pfp = perfluoropinacolyl).
(15) E. R. Falardeau, K. W. Morse, and J. G. Morse, *Inorg. Chem.*, **14**, 1239 (1975): allyltrifluorophosphorane.
(16) N. J. De Ath, D. B. Denney, D. Z. Denney, and Y. F. Hsu, *J. Am. Chem. Soc.*, **98**, 768 (1976): difluorophenylphosphoranes containing four-membered rings.
(17) J. W. Weiss and R. Schmutzler, *J. Chem. Soc., Chem. Commun.*, 643 (1976): 1-$AdPF_4$ (Ad = adamantyl).
(18) C. G. Moreland, G. O. Doak, L. B. Littlefield, N. S. Walker, J. W. Gilje, R. W. Braun, and A. H. Cowley, *J. Am. Chem. Soc.*, **98**, 2161 (1976): Me_2PF_3, Et_2PF_3, $(Me_2N)_2PF_3$.
(19) K. I. The and R. G. Cavell, *Inorg. Chem.*, **15**, 2518 (1976): $(CF_3)_3P(F)Y$ (Y = NMe_2, OMe, SMe, $OSiMe_3$).
(20) A. H. Cowley and R. C. Y. Lee, *J. Chem. Soc., Chem. Commun.*, 111 (1977): $[Me_3Si(Me)N]PF_4$.
(21) K. I. The and R. G. Cavell, *Inorg. Chem.*, **16**, 1463 (1977): $Me(CF_3)_2PXY$ (X, Y = F, Cl, OMe, NMe_2).
(22) J. I. Musher, *J. Am. Chem. Soc.*, **94**, 5662 (1972).
(23) R. S. Berry, *J. Chem. Phys.*, **32**, 933 (1960).
(24) We use the term tetragonal pyramid rather than square pyramid since the four basal ligands are not identical.
(25) I. Ugi, D. Marquarding, H. Klusacek, P. Gillespie, and F. Ramirez, *Acc. Chem. Res.*, **4**, 288 (1971).
(26) R. Hoffmann, J. M. Howell, and E. L. Muetterties, *J. Am. Chem. Soc.*, **94**, 3047 (1972).
(27) P. Russegger and J. Brickmann, *Chem. Phys. Lett.*, **30**, 276 (1975).
(28) A. Strich and A. Veillard, *J. Am. Chem. Soc.*, **95**, 5574 (1973).
(29) J. A. Altmann, K. Yates, and I. G. Csizmadia, *J. Am. Chem. Soc.*, **98**, 1450 (1976).
(30) G. M. Whitesides and H. L. Mitchell, *J. Am. Chem. Soc.*, **91**, 5384 (1969).
(31) R. R. Holmes and J. A. Deiters, *J. Am. Chem. Soc.*, **99**, 3318 (1977).
(32) See, e.g., A. Veillard in "Quantum Mechanics of Molecular Conformations", B. Pullman, Ed., Wiley, London, 1975, p 17.
(33) M. Bénard, A. Dedieu, J. Demuynck, M.-M. Rohmer, A. Strich, and A. Veillard, "Asterix: a System of Programs for the Univac 1110", unpublished work.
(34) B. Roos and P. Siegbahn, *Theor. Chim. Acta*, **17**, 209 (1970).
(35) D. R. Whitman and C. J. Hornback, *J. Chem. Phys.*, **51**, 398 (1969).
(36) A. Veillard, *Theor. Chim. Acta*, **12**, 405 (1968).
(37) S. Huzinaga, *J. Chem. Phys.*, **42**, 1293 (1965).
(38) G. H. F. Diercksen and W. P. Kraemer, *Chem. Phys. Lett.*, **5**, 570 (1970).
(39) J. B. Collins, P. v. R. Schleyer, J. S. Binkley, and J. A. Pople, *J. Chem. Phys.*, **64**, 5142 (1976).
(40) R. R. Holmes and R. N. Storey, *Inorg. Chem.*, **5**, 2146 (1966).
(41) P. M. Treichel, R. A. Goodrich, and S. B. Pierce, *J. Am. Chem. Soc.*, **89**, 2017 (1967).
(42) L. S. Bartell and K. W. Hansen, *Inorg. Chem.*, **4**, 1777 (1965).
(43) (a) E. L. Muetterties, W. Mahler, and R. Schmutzler, *Inorg. Chem.*, **2**, 613 (1963); (b) E. L. Muetterties, W. Mahler, K. J. Packer, and R. Schmutzler, *ibid.*, **3**, 1298 (1964).
(44) R. J. Gillespie, *J. Chem. Educ.*, **47**, 18 (1970).
(45) P. C. Van Der Voorn and R. S. Drago, *J. Am. Chem. Soc.*, **88**, 3255 (1966).
(46) C. Brun, F. Choplin, and G. Kaufmann, *Inorg. Chim. Acta*, **6**, 77 (1972).
(47) A. Rauk, L. C. Allen, and K. Mislow, *J. Am. Chem. Soc.*, **94**, 3035 (1972).
(48) F. Keil and W. Kutzelnigg, *J. Am. Chem. Soc.*, **97**, 3623 (1975).
(49) G. H. F. Diercksen and W. P. Kraemer, *Chem. Phys. Lett.*, **6**, 419 (1970).
(50) P. A. Kollman and L. C. Allen, *Chem. Rev.*, **72**, 283 (1972).
(51) J. D. Dill, L. C. Allen, W. C. Topp, and J. A. Pople, *J. Am. Chem. Soc.*, **97**, 7220 (1975).
(52) L. S. Bernstein, J. J. Kim, K. S. Pitzer, S. Abramowitz, and I. W. Levin, *J. Chem. Phys.*, **62**, 3671 (1975).
(53) L. S. Bernstein, S. Abramowitz, and I. W. Levin, *J. Chem. Phys.*, **64**, 3228 (1976).
(54) See, e.g., M. Menzinger and R. Wolfgang, *Angew. Chem., Int. Ed. Engl.*, **8**, 438 (1969).
(55) R. G. Pearson, "Symmetry Rules for Chemical Reactions-Orbital Topology and Elementary Processes", Wiley, New York, N.Y., 1976, p 191.
(56) The main difference is the position of chlorine in the apicophilicity sequence. First Cavell and co-workers attribute to Cl an apicophilicity equivalent to the one of F, although vibrational, NMR studies (see ref 1b and references therein) and MO calculations[46] indicate that in PCl_nF_{5-n} (n = 1, 4), trigonal-bipyramidal phosphoranes, the axial (=apical) positions are preferentially occupied by the fluorine atoms. Second, on the basis of NMR studies, Cavell and co-workers draw the conclusions that Cl is more apicophilic than CF_3,[10,11,21,57] although vibrational studies on CF_3PCl_4[58] and $(CF_3)_2PCl_3$[59] and recent electron diffraction data on $(CF_3)_2PCl_3$ and $(CF_3)_3PCl_2$[60] suggest the contrary.
(57) D. D. Poulin and R. G. Cavell, *Inorg. Chem.*, **13**, 2324 (1974).
(58) J. E. Griffiths, *J. Chem. Phys.*, **41**, 3510 (1964).
(59) J. E. Griffiths and A. L. Beach, *J. Chem. Phys.*, **44**, 2686 (1966).
(60) H. Oberhammer and J. Grobe, *Z. Naturforsch. B*, **30**, 506 (1975).
(61) H. Yow and L. S. Bartell, *J. Mol. Struct.*, **15**, 209 (1973).
(62) K. W. Hansen and L. S. Bartell, *Inorg. Chem.*, **4**, 1775 (1965).
(63) S. B. Pierce and C. D. Cornwell, *J. Chem. Phys.*, **48**, 2118 (1968).
(64) J. M. Howell, *J. Am. Chem. Soc.*, **97**, 3930 (1975).
(65) D. Britton and J. D. Dunitz, *J. Am. Chem. Soc.*, **97**, 3836 (1975).